This is an accepted manuscript entitled “Mesoscopic Motion of Optically Trapped Particle Synchronized with Photochromic Reactions of Diarylethene Derivatives”, published in *J. Phys. Chem. Lett.*, 9 (**2018**), 2659-2664..

To see the published version, click a link below:

https://pubs.acs.org/doi/abs/10.1021/acs.jpclett.8b00890

Mesoscopic Motion of Optically Trapped Particle Synchronized with Photochromic Reactions of Diarylethene Derivatives

Syoji Ito[1,4], Morio Mitsuishi[1], Kenji Setoura[1], Mamoru Tamura[3,4], Takuya Iida[3,4], Masakazu Morimoto[2], Masahiro Irie[2], and Hiroshi Miyasaka[1]**

1 Division of Frontier Materials Science and Center for Promotion of Advanced Interdisciplinary Research, Graduate School of Engineering Science, Osaka University, Toyonaka, Osaka 560-8531, Japan

2 Department of Chemistry and Research Center for Smart Molecules, Rikkyo University, Nishi-Ikebukuro 3-34-1, Toshima-ku, Tokyo, 171-8501, Japan

3 Department of Physical Science, Graduate School of Science, Osaka Prefecture University, 1-1, Gakuen-cho, Nakaku, Sakai, Osaka 599-8531, Japan.

4 Research Institute for Light-induced Acceleration System (RILACS), Osaka Prefecture University Sakai 599-8570, Japan.

Corresponding Author

* sito@chem.es.osaka-u.ac.jp. * miyasaka@chem.es.osaka-u.ac.jp.

ABSTRACT Not only the energy but also the momentum of photons transfers to material via photo-absorption; this momentum transfer, known as radiation pressure, can induce motions of small particles. It can therefore be expected to induce mechanical motions of mesoscopic materials synchronized with the reversible change of their absorption coefficient by external stimuli. In the study, we demonstrated quantitative photomechanical motions in mesoscopic regions by combining optical tweezer and photochromic reactions of diarylethene (DAE). A microparticle including DAE was optically trapped with 532-nm laser and the absorption band of the DAE was photo-switched with UV laser, resulting in the modulation of the radiation force through the change in the complex dielectric constant of the particle. In this process, mesoscopic mechanical motions were successfully induced by the photochromic reaction. The present approach is potentially applicable in a wide variety of nano/micro-mechanical devices, and also paves the way to detecting the photoabsorption for molecules via photomechanical response.

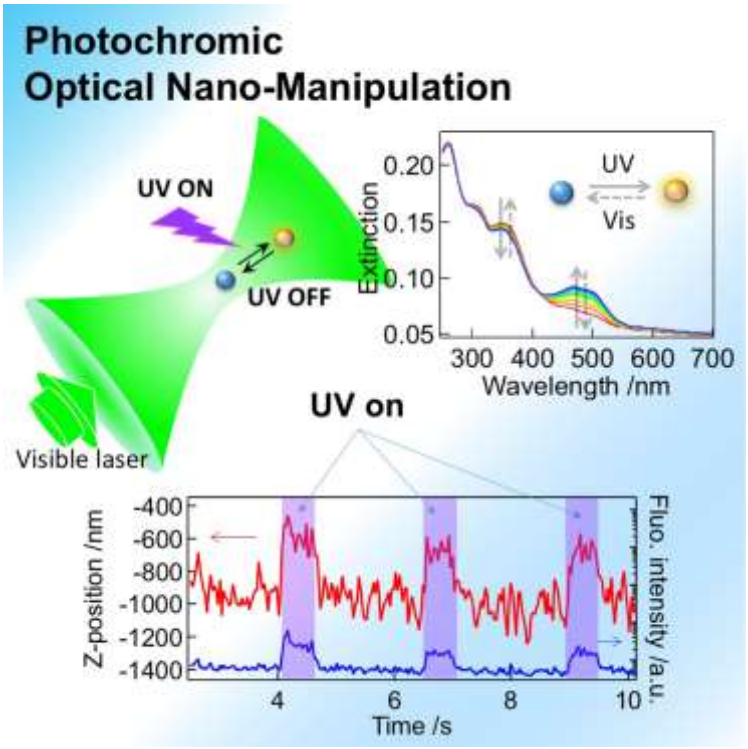
Photochromic
Optical Nano-Manipulation
UV ON
UV OFF
Visible laser
Extinction
0.20
0.15
0.10
0.05
300 400 500 600 700
Wavelength /nm
UV
Vis
UV on
Z-position /nm
-400
-600
-800
-1000
-1200
-1400
4
6
8
10
Time /s
Fluo. intensity /a.u.

Resonant absorption of photons plays a significant role as an initial step of a number of photofunctional processes in natural and artificial systems where the energy of photons is converted to the electronically excited state and utilized in the subsequent chemical reactions and physical processes. Not only the energy but also the momentum of photons is, in general, resonantly transferred to material through photo-absorption.[1,2,3,4] This momentum transfer is one of origins of radiation pressure affecting motions of tiny materials under photo-irradiation. The force arising from the resonant absorption induces the motion of the materials towards the direction of light propagation. In addition to the absorption force, scattering and gradient forces also contribute to radiation pressure. While the direction of the absorption and scattering forces is along the Poynting vector of incident light, the gradient force keeps tiny materials at the focal point of the incident light. In the case where the gradient force is dominant, we can utilize this force in the manipulation of tiny materials ranging from ca. 10 nm – 10 μm; this is known as laser trapping or optical tweezer.

Chemical reactions are generally accompanied with the change of the resonant absorption band of molecules, because the structure of electronic states is dependent on molecular structure and its constituent atoms. Accordingly, chemical reactions occurring in a tiny object can modulate the radiation pressure acting on the object through the change of absorption and scattering cross-sections. As introduced above, the gradient force keeps a small object at the focal point of incident light, while the direction of the absorption and scattering forces is along the axis of the light propagation. Hence, the chemical reaction in a tiny material can potentially induce its mechanical motions under laser trapping.

Photochromic molecules undergo reversible isomerization reactions between isomers with different resonant absorption bands.[5,6,7,8,9] Switching of the color through the photochemical

reaction modulates the absorption and scattering forces and, consequently, can induce the reversible motion synchronizing with the colorization and decolorization reactions. This can provide a new method to control the motion of materials in mesoscopic scales. Along this line, we have investigated the photoresponses of tiny polymer particles including a photochromic diarylethene derivative under laser trapping.[10] Reversible motions with a few 100-nm to a few-μm displacement, synchronizing with the photochromic reactions, were experimentally observed and these movements were rationally accounted for by the theoretical calculation with the absorption change of the quite small number of molecules (10^{-18} mol). The present result is potentially applicable to a wide variety of nano/micro-mechanical devices with versatile motions through the photochemical reactions regulated by light irradiation.

Small particles of poly(methyl methacrylate) (PMMA) with a fluorescent diarylethene derivative[11] were prepared as a specimen. 300-nm sized (in diameter) PMMA particles provided by SEKISUI PLASTICS (XX-3832Z) were used as received. The particles were immersed in 1,4-dioxane (Wako, 045-24491) solutions of a fluorescent diarylethene derivative, **DE1**, at a concentration of 8.5×10^{-4} M. The stock solutions were kept in a dark area in an experimental room at a temperature of 296K for 48 hours, leading to the inclusion of the open-ring isomers of the diarylethene into the PMMA particles with solvent molecules by swelling. The particles including **DE1** were separated from the solution by centrifugation, then dispersed into water prepared with an ultrapure water system (DirectQ UV, Millipore).

Chemical structures of the open- and closed-ring isomers of **DE1** are shown in Figure 1a. Figure 1b and 1c show absorption and fluorescence spectra of **DE1** in 1,4-dioxane solution. UV irradiation of the nonfluorescent open-ring isomer, **DE1(o)**, yields the highly fluorescent closed-ring isomer, **DE1(c)**, with the cyclization yield of 0.62. The closed-ring isomer excited by the

visible light undergoes the radiative transition with a fluorescence quantum yield of 0.88 in completion with the cycloreversion reaction with a low reaction quantum yield (1.8×10^{-4}).

Figure 1d shows absorption spectra of colloidal suspension of the PMMA particles containing **DE1**. Although the scattering signal overlaps on the absorption spectrum, the absorption maxima and spectral band shape before the UV irradiation are almost the same with those of **DE1(o)** in 1,4-dioxane solution. After the 355-nm irradiation for 10 min, the absorption band in the visible region ascribable to **DE1(c)** appears as shown in Figure 1d. Fluorescence spectrum of the PMMA particle after the UV irradiation is shown in Figure 1e, where the particle was excited with a CW 532-nm laser and an optical long-pass filter >535 nm was introduced to avoid the scattering signal of the 532-nm laser light. As is clearly shown in this figure, the emission maximum and spectral band shapes are almost the same with those of **DE1(c)** in 1,4-dioxane solution. This result clearly indicates that the cyclization reaction, **DE1(o)** → **DE1(c)**, can take place in the solid PMMA environment, which is consistent with previous studies demonstrating the photochromic reactions of DAE in solids.[6, 9]

A drop of the colloidal suspension of the PMMA particles was injected into a 30-μL sample chamber consisting of two well-cleaned coverslips (Matsunami, 24 × 32 × 0.17 mm) and a 300-μm thick silicon-rubber sheet with a hole. Details of the cleaning process of the cover slips were described previously.[12] A single PMMA particle with **DE1** was optically trapped with a CW visible (532 nm) laser and the photochromic reaction was induced by photoirradiation with a CW UV (355 nm) laser. The details of the optical setup are described in the supporting information **S1**.

For precise detection of the three-dimensional motion of a trapped particle, we employed astigmatism imaging method,[13,14] where the position of a fluorescent particle along the optical

axis (Z-axis) is obtained by the analysis of the aspect ratio of the fluorescent image. The Z-position of a trapped particle is dependent on the gradient, scattering, and absorption forces. The number of colored **DE1(c)**, which can be changed by the photochromic reaction, mainly affects the absorption and scattering forces, leading to the Z-displacement of the particle as shown in Figure 1f. The details of the radiation force acting on the particle through the UV irradiation cycle is schematically illustrated in Figure S4 in the supporting information **S6**.

Figure 1g shows the fluorescence image of a PMMA particle in water under the trapping by the 532-nm laser with a power of 6 mW at the particle position. In this measurement, optical setup for the astigmatism imaging was employed. Upon irradiation with weak 355 nm light (typically < 130 nW) to the trapped particle the very weak background emission or scattering image of the particle (Figure 1g (i)) dramatically increased as shown in Figure 1g (ii). This increase is due to the formation of fluorescent closed-ring isomers in the particle. The bright image again returned to the weak image under irradiation with the 532-nm laser (Figure 1g (iii)).

In addition to the change of the fluorescence intensity, Figure 1g also shows the change of the aspect ratio of the fluorescence image by the UV irradiation at 355 nm. This result indicates that the position along the Z-axis under the laser trapping is affected by the irradiation at 355 nm. Details on the setup for 3D tracking and the quantitative information on the tracking accuracy (typically 20 nm WFHM) along the Z-axis are shown in the supporting information **S2** and **S3**.

Figure 1h shows the position along the Z-axis and the fluorescence intensity of the trapped particle under the repetitive irradiation of the UV light (0.5 s for each exposure). Because the particle was continuously irradiated with the 532-nm laser, the cycloreversion reaction, **DE1(c)** → **DE1(o)**, was dominantly induced under the laser trapping at 532 nm. This figure clearly shows that the Z-position of the particle is modulated by the UV irradiation; Z-displacement of

ca. 250 - 300 nm toward the propagation direction of the 532-nm laser light was induced for the trapped particle by the irradiation with the UV laser at 29 Wcm^{-2} (36 nW). The repeatable Z-displacement could be induced at least 10 times by the UV irradiation although the fluorescence intensity of the particle gradually decreased, which is probably due to the photodegradation of DAEs under the intense visible light irradiation at 532 nm (typically 2 - 3 $MWcm^{-2}$).

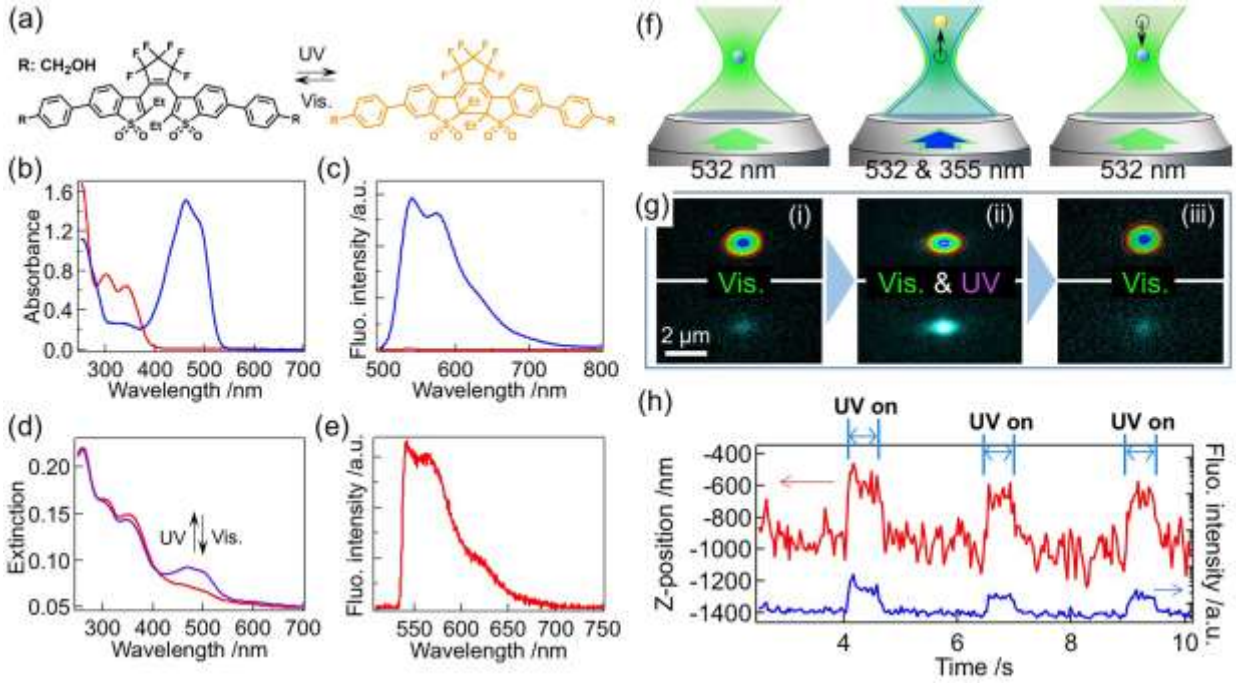

Figure 1. (a) Photochromic reactions of the diarylethene derivative **DE1** used in the present study. (b) Steady-state absorption spectrum of (red) the open-ring isomer and (blue) closed-ring isomer of **DE1** in 1,4-dioxane solution. (c) Fluorescence spectrum of the closed-ring isomer in 1,4-dioxane solution photoexcited at 488 nm (d) Absorption spectra of colloidal suspension of the PMMA particles containing **DE1**. Spectrum before the irradiation with the 355-nm light and that after irradiation for 10 min. (e) Fluorescence spectrum of PMMA particles containing **DE1** on a cover slip in the air, irradiated with a CW 532-nm laser. An optical long-pass filter > 540 nm was introduced to avoid the scattering signal of the 532-nm laser light. (f) Schematic

illustration of the photo-switching of radiation force by using photochromic reaction. (g) Fluorescence images of a trapped PMMA particle containing **DE1** upon photoirradiation: (i) and (iii) only with the 532-nm laser at 6 mW and (ii) with the UV (355 nm, 29 Wcm^{-2}) and the visible (532 nm, 5 mW) lasers. The contour plots in the upper side show the fitting results with 2D Gaussian. (h) Time course of the positional change along the Z-axis (red line) and the fluorescence intensity (blue line) of a trapped particle with the CW 532-nm laser with 6 mW. The trapped particle was periodically photo-irradiated with the CW UV laser light with an irradiation time of 0.5 s.

To quantitatively characterize the Z-displacement under the UV irradiation, we estimated gradient, scattering, and absorption forces acting on a trapped particle. First, so as to calculate gradient force under the present trapping condition, the shape and depth of optical trapping potential were experimentally determined. For the measurement of the shape of trapping potential corresponding to the intensity distribution of the 532-nm light, we obtained a stage-scanning confocal micrograph of a single quantum dot on a cover slip under the 532-nm photoexcitation. The spot size of the green laser was estimated to be ca. 0.24 μm as $1/e^2$ radius on the focal (XY) plane and 1.33 μm as $1/e^2$ half-width (See supporting information **S4** for the details) along the Z-direction.

Next, for the estimation of trapping potential depth, the positon of optically trapped single PMMA particle on the XY plane was tracked by means of localization method. Figure 2a shows a trajectory of the Brownian motion of a trapped PMMA particle on the XY plane,[15,16,17] indicating that the PMMA particle was confined in a circular area with a diameter of ca. 150 nm.

Time course of the X-position of the trapped particle is shown in Figure 2b and the histogram of the X-position obtained from Figure 2b is exhibited in Figure 2c. The blue line in Figure 2c shows the analytical result with Gauss function.

To estimate the depth of gradient-force trapping potential under the present experimental condition from the data of single particle tracking shown in Figures 2a-2c, we conducted Brownian dynamics simulation (BDS). The random movements of a trapped particle in solution can be reproduced by the BDS using the algorithm of which bases were developed by Ermak and McCammon.[18] In this simulation, solvent was regarded as continuum medium, then motions of individual solvent molecules nor their interactions with the surface of trapped particles were not considered. Detailed calculation process for the motion of a particles under optical gradient force is described in our previous report.[19] Figures 2d-2f show an example of calculation result on Brownian motion of a trapped PMMA particle with a 300-nm diameter in water at 295 K. In this simulation, the experimentally obtained spot size of trapping laser beam (240 nm in radius, described in supporting information **S4**) was employed. Figure 2d shows the trajectory of the Brownian motion of a trapped 300-nm PMMA particle on the focal (XY) plane of the objective under a trapping potential depth of 99 k_BT. Figures 2e and 2f respectively show corresponding time course of the X-position of the trapped 300-nm particle and its distribution obtained through the simulation. By analyzing the distribution with Gauss function, we obtained the width (1/e width) of the positional fluctuation of a trapped particle. A series of simulation under different trapping potential depths and successive analysis in the aforementioned manner provided the relation between the width of positional fluctuation along the X-axis and trapping potential depth as shown in Figure 2g. By comparing the Gauss width (1/e width) of the distribution (41.9 nm) with the computational results of BDS (Figure 2d-2g), the depth of trapping potential by the

gradient force was estimated to be 99 k_BT for incident laser power of 5 mW. Here, k_B and T are the Boltzmann constant and Kelvin temperature, respectively.

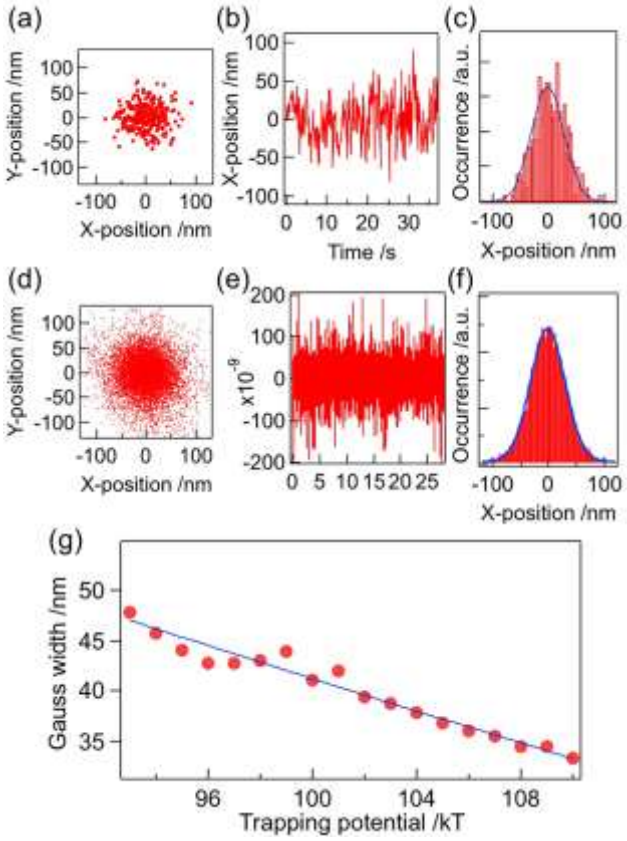

Figure 2. (a) Distribution of the XY-position of a PMMA particle trapped in water with the 532-nm laser at 5-mW incident power at every 122 ms. (b) The time-course of positional fluctuation along the X-axis of the trapped PMMA particle. (c) Histogram of the X-position for the time trajectory shown in (b). The solid line is the curve obtained by the analysis with a Gauss function. (d) Distribution of the XY-position of a PMMA particle trapped in water at every 2 ms in gradient-force trapping potential with a depth of 99 k_BT in the presence of scattering force (simulation result). (e) The time-course of positional fluctuation along the X-axis of the trapped particle shown in (d). (f) Histogram of the X-position for the time trajectory shown in (e). (g) The 1/e half-width of the distributions of X-displacement as a function of optical trapping

potential depth; this plot was obtained from computational results on the basis of Brownian dynamics simulation.

The gradient force was directly calculated by differentiating the optical trapping potential obtained in the aforementioned manner. On the other hand, the scattering and absorption forces, F_{Sct} and F_{Abs}, by the UV and VIS lasers were calculated by using equations 1 and 2.

$$F_{Sct}(\lambda) = \frac{n_m}{c} C_{Sct}(\lambda)\ I(\lambda) \qquad (1)$$

$$F_{Abs}(\lambda) = \frac{n_m}{c} N C_{Abs}(\lambda)\ I(\lambda) \qquad (2)$$

Here, $C_{\mathrm{Sct}}(\lambda)$ is the scattering cross-section of single PMMA particle, while $C_{\mathrm{Abs}}(\lambda)$ and N are the absorption cross-section for single **DE1** molecule and the number of **DE1** molecule in a PMMA particle, respectively. $I(\lambda)$, n_{m}, c, and λ are the input laser intensity, the refractive index of surrounding medium, the speed of light in vacuum, and the wavelength of light respectively. The scattering and absorption cross-sections of the PMMA particle were calculated by using finite-difference time-domain (FDTD) method under effective medium approximation with the help of Mie theory[20,21,22]. The calculated value of $C_{\mathrm{Abs}}(\lambda)$ per DAE molecule exhibited good agreement with the absorption cross-section of single DAE molecule calculated from the molar absorption coefficient of the DAE in 1,4-dioxane.[23] Details of the calculation and results are shown in the supporting information **S5**.

The net radiation force due to the photon momentum transfer is the sum of the scattering and absorption forces due to the radiative and nonradiative dissipation process,[24,25] the summation of two forces, $F_{Sct}(\lambda) + F_{Abs}(\lambda)$, by the UV and VIS lasers was calculated by using equation 3.

$$F_{Sct}(\lambda) + F_{Abs}(\lambda) = \frac{n_m}{c} C_{Ext}(\lambda,\ N_c)\ I(\lambda) \qquad (3)$$

Here, N_c is the number of **DE1(c)** in single PMMA particle and $C_{Ext}(\lambda, N_c)$ is the extinction cross-section of single PMMA particle as a function of N_c and λ. We estimated the complex refractive index of PMMA particle with **DE1(c)**, and calculated the $C_{Ext}(\lambda, N_c)$ for the arbitrary N_c value as shown in the supporting information **S5**.

Figure 3a shows the sum of gradient, scattering, and absorption forces acting on a PMMA particle under the gradient-force trapping potential of 119 k_BT (corresponding to 6 mW trapping laser power) as a function of the Z-position. The N_c in the figure is the numbers of the closed-ring isomers in the PMMA particle. It should be noted here that only the photon forces by the 532-nm light are taken into consideration because the contribution of the UV light is negligible owing to its very low intensity (7.8 - 130 Wcm^{-2}) at the specimen. The increase in the scattering cross-section of the PMMA particles was in the same order of the increase in the absorption cross-section at 532 nm (see supporting information **S5**). Hence both contributions were taken into account in the calculation.

From the result shown in Figure 3a, we obtained the relation between Z-displacement, Δz, and the number of the closed-ring isomer converted from the open form, N_c in a PMMA particle by UV irradiation. In the optical configuration considered in this calculation, Δz does not show the dependence on the incident power of the 532-nm laser, because the increase in trapping stiffness with increasing 532-nm laser power countervails the increase in the sum of absorption and scattering forces. Figure 3b shows a precise plot of the sum of gradient, scattering, and absorption forces along the Z-axis as a function of the Z-position for PMMA particles trapped at three different gradient-force trapping potentials, 79, 99 and 119 k_BT (corresponding to 4, 5, and 6 mW incident powers at 532 nm), for two different *Nc*, 2.0×10^4 and 1.5×10^5. The figure clearly

demonstrates that the same Δz for the three laser powers at a same N_c. In other words, Δz depends only on incident UV power but not 532-nm laser power as shown in Figure 3c, the relation between Δz and N_c for the three trapping potential depths.

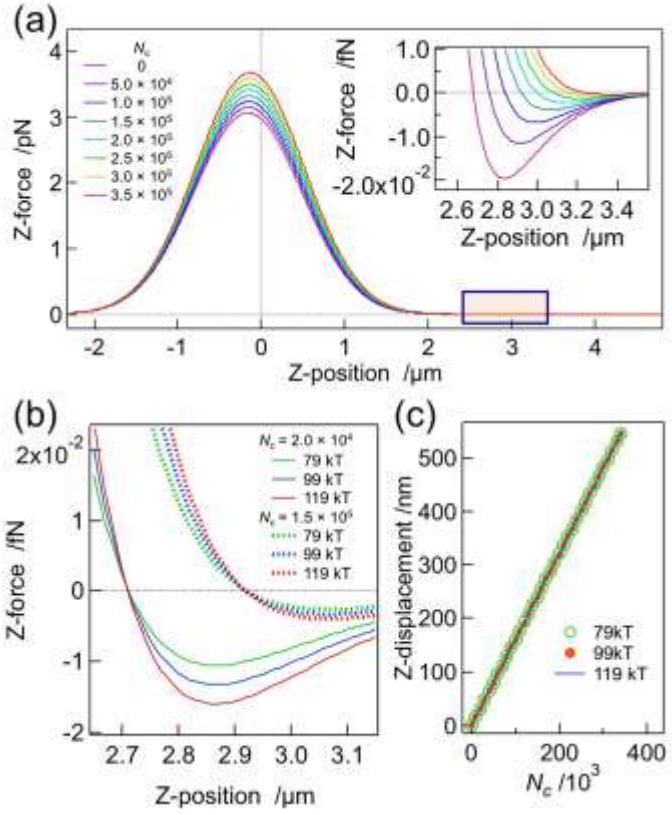

Figure 3. (a) Optical force (the sum of gradient, scattering, and absorption forces) along the Z-axis acting on a PMMA particle under trapping potential of 119 k_BT (6 mW incident power), calculated as a function of the number of the closed-ring isomers in a particle. The right inset is a precise plot in the Z-position ranging from 2.5 to 3.5 μm shown as a blue rectangle in the main plot. (b) The sum of gradient, scattering and absorption forces along the Z-axis acting on a PMMA particle under trapping potential of 79, 99 and 119 k_BT for $N_c = 2.0\times10^4$ and 1.5×10^5. (c)

Relation between the Z-displacement of a trapped particle and N_c for the three trapping potential depths.

Figure 4 shows experimentally obtained Δz for a particle trapped with the 532-nm light at 4 and 6 mW laser powers as a function of UV intensity. In the analysis, Z-displacement only in the first several cycles were analyzed, where each Z-displacement showed comparable value, so that the effect of photodegradation is not involved. The Z-displacement monotonically increases with increasing UV power with saturation in the high light intensity region. This can be ascribed to the saturation of the increase in N_c (see the supporting information **S7** showing detailed calculation of N_c as a function of the UV intensity). Comparing the experimental results with the calculation (Figure 3c) leads to the quantitative estimation of the number of photo-isomerized DAEs in a PMMA particle; the relation between Δz and N_c is summarized in Table 1 for the trapping laser power of 4 and 6 mW. Under the present condition, the photoinduced conversion of 8.1 - 9.8×10^4 DAE molecules to the closed-ring isomer resulted in 130 - 160 nm displacement along the Z-axis. In other words, the degree of photochemical reaction at the 10^{-18} mole level can be monitored by the measurement of photomechanical response of the particle.

Figure 3b and 3c predicted that Δz does not depend on incident 532-nm laser power but only on the incident UV power. The plots of Δz in Figure 4 are in line with the expectation; Δz shows almost same behavior with increasing N_c for 4 and 6-mW incident 532-nm power. However, the value of Δz is slightly different between the two photoirradiation conditions. The values of Δz at 4-mW incident power are always 10-20% smaller than those at 6-mW incident power. The difference is systematic and not negligible. This small difference is ascribed to the different

number of absorbed and scattered 532-nm photons by a particle undergoing thermal fluctuation at the bottom of the gradient-force trapping potential. The inset of Figure 4 shows the positional fluctuation of trapped PMMA particle along the X-axis as histograms (simulation results). The simulation result indicates that a particle under shallower trapping potential (79 k_BT) has more chance to move out to a surrounding area of the focal spot of 532-nm laser, where the particle experiences lower light intensity than on the optical axis. As a result, the particle trapped by the 4-mw incident power experienced absorption and scattering forces slightly lower that those under trapping with the 6-mW incident power.

In the report, we have demonstrated the photo-switching of radiation forces acting on a microparticle by using photochromic reactions of **DE1**. The photoinduced mechanical motions of organic systems is potentially applicable in a wide variety of micromechanical devices. In addition, this approach also paves the way to monitoring the absorption of photons by small number of molecules by detecting photomechanical response. We foresee the approach proposed in the report provides a new avenue of photon-controlled opto-mechanical response of organic systems as well as a new absorption spectroscopy for small number of molecules. To control further complicated and elaborate mechanical motions, different photo-irradiation conditions and different molecular systems are under investigation.

Table 1. Z-displacement of trapped PMMA particles and the number of **DE1(c)** photo-converted by UV irradiation in a PMMA particle, N_c .

UV intensity /Wcm^{-2}	Trapping laser power 4mW		Trapping laser power 6mW	
	Z-displacement, Δz /nm	*N*c	Z-displacement, Δz /nm	*N*c
7.8	130	8.1×10^4	160	9.8×10^4
13	240	1.5×10^5	270	1.7×10^5
29	280	1.8×10^5	320	2.0×10^5
52	330	2.1×10^5	380	2.3×10^5
130	380	2.3×10^5	430	2.7×10^5

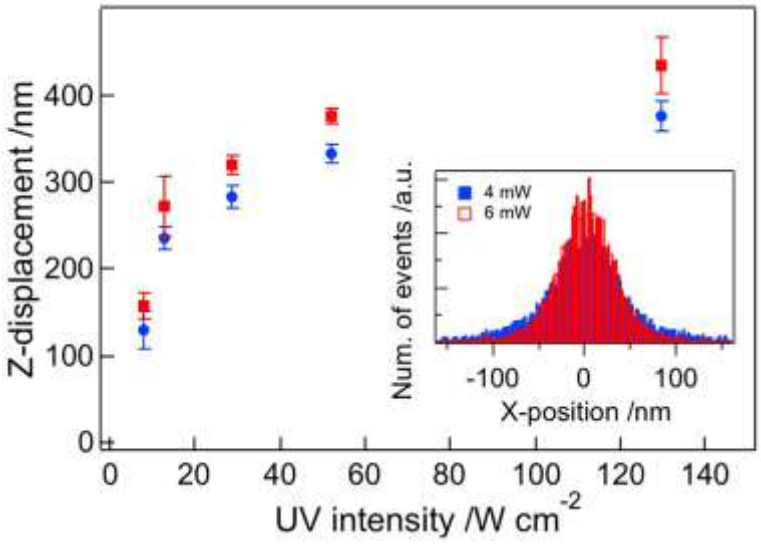

Figure 4. Plot of the Z-displacement of a particle under trapping potential of (blue solid circle) 79 and (red solid square) 119 k_BT (4 and 6 mW incident power, respectively) as a function of UV laser power (experimental data). (Inset) Histograms of the X-position of PMMA particle

(simulation result) under optical trapping with (blue) 4 and (red) 6 mW incident laser powers at 532 nm without UV light.

ACKNOWLEDGMENT

This work was supported by JSPS KAKENHI Grant Numbers JP16H06505 and 16H06507 in Scientific Research on Innovative Areas “Nano-Material Optical-Manipulation”, JP26107002 and JP15H01096 in Scientific Research on Innovative Areas "Photosynergetics", JP26288009, JP16H03827, JP15K13625 and JP17H00856 and Key Project Grant Program of Osaka Prefecture University.

Supporting Information Available: S1. Optical setup for laser trapping, S2. Three-dimensional single-particle tracking, S3. Photoswitching behavior of DE1 in a 300-nm PMMA particle and fluorescence intensity dependence of position-determination accuracy along the Z-axis, S4. Estimation of the spot size of the 532-nm laser light focused by the microscope objective with NA 1.35, S5. Calculation of extinction spectrum and refractive index of single PMMA particle including DE1, S6. Radiation forces acting on an optically trapped PMMA particle with DE1, S7. Concentration of the closed-ring isomer of DE1 as a function of UV intensity. This material is available free of charge via the Internet at http://pubs.acs.org.

Author Contributions

S.I., M. Mitsuishi, and K.S. performed experiments and analyses of optical trapping. M. Morimoto and M. I. prepared and evaluated the samples. M. T. and T. I. conducted numerical calculations. S.I. and H.M. designed the concept of the present work. S.I. and H.M. prepared the manuscript and, discussed about it with all authors. All authors have given approval to the final version of the manuscript.

Notes

The authors declare no competing financial interest.

REFERENCES

(1) Lebedev, P. N. Untersuchungen über die Druckkräfte des Lichtes. *Annalen der Physik. Leipzig* **1901**, 6, 433-458.

(2) Nichols, E.F.; Hull, G. F. The Pressure due to Radiation. *Phys. Rev.* **1903**, 17, 26-50.

(3) Chu, S. Laser Manipulation of Atoms and Particles. *Science* **1991**, 253, 861-866.

(4) Ashkin A. History of Optical Trapping and Manipulation of Small-neutral Particle, Atoms, and Molecules. *IEEE J. Sel. Top. Quantum Electron.* **2000,** 6, 841–856.

(5) Brown, G. H. *Photochromism* (Wiley-Interscience, New York, 1971).

(6) Irie, M.; Fukaminato, T.; Matsuda, K.; Kobatake, S. Photochromism of Diarylethene Molecules and Crystals: Memories, Switches, and Actuators. *Chem. Rev.* **2014**, 114, 12174-

12277.

(7) Waldeck, D. H. Photoisomerization Dynamics of Stilbenes. *Chem. Rev.* **1991**, 91, 415-436.

(8) Irie, M.; Mohri, M. Thermally Irreversible Photochromic Systems. Reversible photocyclization of diarylethene derivatives. *J. Org. Chem*. **1988**, 53, 803-808.

(9) Irie, M. Diarylethenes for Memories and Switches. *Chem. Rev*. **2000**, 100, 1685-1716.

(10) Ashkin, A.; Dziedzic, J. M.; Bjorkholm, J. E.; Chu, S. Observation of a Single-Beam Gradient Force Optical Trap for Dielectric Particle. *Opt. Lett*. **1986**, 11, 288-290.

(11) Uno, K.; Niikura, H.; Morimoto, M.; Ishibashi, Y.; Miyasaka, H.; Irie, M. In Situ Preparation of Highly Fluorescent Dyes upon Photoirradiation. *J. Am. Chem. Soc*. **2011**, 133, 13558-13564.

(12) Setoura, K.; Ito, S.; Miyasaka, H. Stationary Bubble Formation and Marangoni Convection Induced by CW Laser Heating of a Single Gold Nanoparticle. *Nanoscale* **2017**, 9, 719-730.

(13) Huang, B.; Wang, W.; Bates, M.; Zhuang, X. Three-Dimensional Super-Resolution Imaging by Stochastic Optical Reconstruction Microscopy. *Science* **2008**, 319, 810-813.

(14) Ito, S.; Taga, Y.; Hiratsuka, K.; Takei, S.; Kitagawa, D.; Kobatake, S.; Miyasaka, H. Restricted Diffusion of Guest Molecules in Polymer Thin Films on Solid Substrates as Revealed by Three-Dimensional Single-Molecule Tracking. *Chem. Commun*. **2015**, 51, 13756-13759.

(15) Gelles, J.; Schnapp, B. J.; Sheetz, M. P. Tracking Kinesin-Driven Movements with Nanometre-Scale Precision. *Nature* **1988**, 311, 450-453.

(16) Qian, H.; Sheetz, M. P.; Elson, E. L. Single Particle Tracking. Analysis of Diffusion and Flow in Two-Dimensional Systems. *Biophys. J*. **1991**, 60, 910-921.

(17) Ito, S.; Kusumi, T.; Takei, S.; Miyasaka, H. Diffusion Processes of Single Fluorescent Molecules in a Polymer-Based Thin Material with Three-Dimensional Network. *Chem.*

Commun. **2009**, 6165-6167.

(18) Ermak, D. L.; McCammon, J. A. Brownian Dynamics with Hydrodynamic Interactions. *J. Chem. Phys.* **1978**, 69, 1352-1360.

(19) Ito, S.; Toitani, N.; Yamauchi, H.; Miyasaka, H. Evaluation of Radiation Force Acting on Macromolecules by Combination of Brownian Dynamics Simulation with Fluorescence Correlation Spectroscopy. *Phys. Rev. E* **2010**, 81, 061402(1-8).

(20) Mie, G. Beiträge zur Optik trüber Medien, speziell kolloidaler Metallösungen. *Ann. Phys*. **1908**, 25, 377-445 (1908).

(21) Bohren, C. F.; Huffman, D. R. *Absorption and Scattering of Light by Small Particles* (Wiley-VCH, New York, 1983).

(22) Setoura, K.; Werner, D.; Hashimoto, S. Optical Scattering Spectral Thermometry and Refractometry of a Single Gold Nanoparticle under CW Laser Excitation. *J. Phys. Chem. C* **2012**, 116, 15458-15466.

(23) Birks, J. B. *Photophysics of Aromatic Molecules* (Wiley-Interscience, New York, 1970).

(24) Iida, T.; Ishihara, H. Force Control between Quantum Dots by Light in Polaritonic Molecule States. *Phys. Rev. Lett.* **2006**, 97, 117402(1-4).

(25) Iida, T.; Ishihara, H. Theory of Resonant Radiation Force Exerted on Nanostructures by Optical Excitation of Their Quantum States: From Microscopic to Macroscopic Descriptions. *Phys. Rev. B* **2008**, 77, 245319(1-16).